

# Construction of an ELS–LEED: an electron energy-loss spectrometer with electrostatic two-dimensional angular scanning

Tadaaki Nagao\* and Shuji Hasegawa

Department of Physics, Graduate School of Science, University of Tokyo, 7-3-1 Hongo, Bunkyo-ku, Tokyo 113-0033, Japan, and Core Research for Evolutional Science and Technology (CREST), Japan Science and Technology Corporation (JST), 4-1-8 Honcho, Kawaguchi, Saitama 332-0012, Japan

A new version of an energy-loss spectrometer with low-energy electron diffraction (ELS–LEED, Henzler type EELS) has been constructed. Different from the prototype spectrometer, which is equipped with a single-pass 127° cylindrical deflector analyser, the present spectrometer consists of an Ibach-type double-pass monochromator, an enlarged single-pass analyser and some magnetic lenses in acceleration and deceleration lenses and in the electrostatic deflection unit for high-resolution LEED. As a preliminary result, with the Si(111)-7 × 7 surface, the present spectrometer showed an energy width (full width at half-maximum) of 18 meV at the quasi-elastic peak and a transfer width of 960 Å at the (00) diffraction spot. Copyright © 2000 John Wiley & Sons, Ltd.

KEYWORDS: electron energy-loss spectroscopy (EELS); low-energy electron diffraction (LEED); energy-loss spectrometer with low-energy electron diffraction (ELS–LEED); high-resolution electron energy-loss spectroscopy (HREELS); high-resolution low-energy electron diffraction (HRLEED); spot profile analysis low-energy electron diffraction (SPA–LEED)

## INTRODUCTION

Energy-loss spectroscopy and diffraction techniques with slow electrons have been applied extensively in surface analysis in the past two decades. The excellent surface sensitivity gives access to information about structures and electronic or vibronic properties at atomic layers in the vicinity of the surface.<sup>1–5</sup> Among these techniques, high-resolution electron energy-loss spectroscopy (HREELS) showed its power and versatility in studying localized vibrational modes, phonon dispersion and dielectric response, not only at the surface but also at an interface several nanometres below the surface.<sup>5–13</sup> High-resolution low-energy electron diffraction (HRLEED) has also enjoyed extensive application to studies ranging from quantitative defect analysis to the study of dynamic scaling during the growth and phase transitions of epitaxial ultrathin films and surface superstructures.<sup>4,14,15</sup> Recently, Henzler *et al.* have developed a unique instrument that is capable of performing HRLEED analysis using electrons monochromatized in the meV regime;<sup>16</sup> an energy-loss spectrometer with low-energy electron diffraction (ELS–LEED). In the electron energy loss spectroscopy (EELS) mode, thanks to its high momentum resolution, the spectrometer has successfully detected new plasmon modes that are difficult to probe by the conventional HREELS technique.<sup>17</sup> Also, by combining

EELS measurements with low-energy electron diffraction (LEED) spot profile analysis, the influence of nanomorphology on the plasma waves in the ultrathin film has been studied in detail.<sup>18</sup> These studies have opened up an exciting new prospect of inspecting nanoscopic transport phenomena in conjunction with plasma waves in low-dimensional or nanostructured materials.

In the present study, we report on the construction of a different version of an ELS–LEED that adopts a double-pass monochromator, which is more difficult in operation but is expected to show high current and narrower energy width at the same time.<sup>19</sup> The design of the EELS part is the same as that by Nagao *et al.*,<sup>20</sup> but with some modifications in the slits and in the acceleration and deceleration lenses.

## DESIGN AND TEST RUNNING

The spectrometer design and the preliminary results in the first test running are described below.

Figure 1 shows a schematic illustration of the new spectrometer. The main components of the spectrometer are as follows: an octopole electrostatic deflector for high-resolution LEED; an Ibach-type monochromator with a double-pass cylindrical deflector analyser (CDA); an energy analyzer with a single-pass CDA; and acceleration and deceleration lenses that transfer the electron beams between the octopole part and the EELS part of the system.

The octopole deflector, which is made out of three sets of eight electrodes, is a component of the spot profile analysis low-energy electron diffraction (SPA–LEED; commercially available from Omicron Vakuumphysik GmbH). All the electrodes in the octopole deflector facing the electron trajectories are coated with colloidal graphite (Dag

\* Correspondence to: T. Nagao, Department of Physics, Graduate School of Science, University of Tokyo, 7-3-1 Hongo, Bunkyo-ku, Tokyo 113-0033, Japan.

E-mail: nagao@phys.s.u-tokyo.ac.jp

Contract/grant sponsor: Ministry of Education, Science, Culture & Sports, Japan; Contract/grant number: 08NP1201.

Contract/grant sponsor: Nippon Sheet Glass Foundation for Materials Science and Engineering.

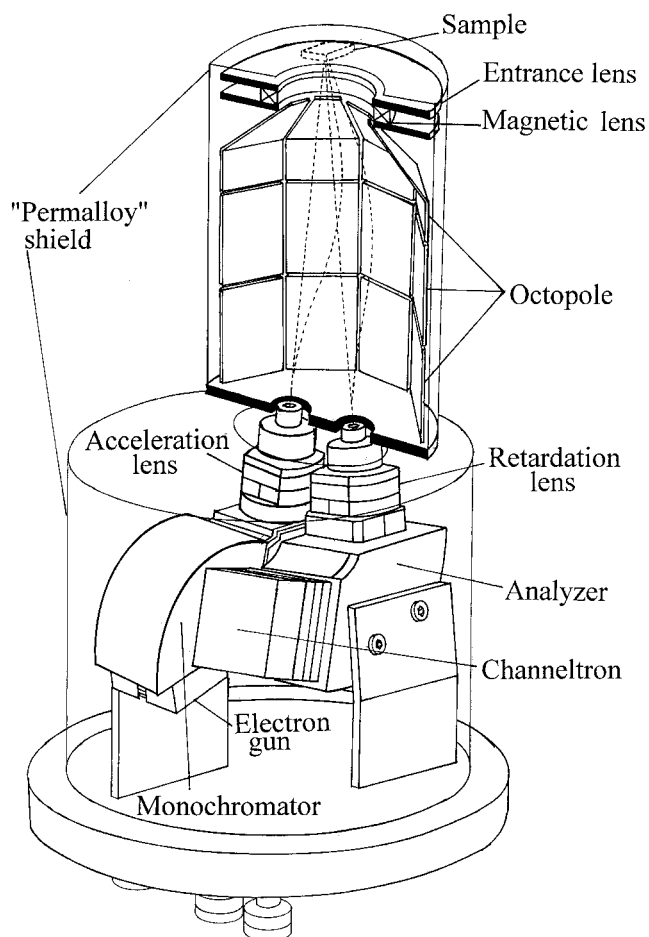


**Figure 1.** Schematic illustration of the new ELS-LEED. The spectrometer is mounted on an ICF306 flange.

154: Acheson) to reduce the secondary electron emission from the electrodes.

The CDAs in the EELS part (monochromator and energy analyser) are made of copper, and all the slits are made of copper-beryllium alloy. All the other components are made of non-magnetic materials such as tantalum, molybdenum and high-purity (99.5%) alumina. We have mechanically polished all the electrodes in the EELS parts and coated them with Dag 154 after depositing gold in vacuum. All the geometrical parameters are the same as in Ref. 20, except that the widths of the slits are magnified by a factor of 1.5. This is to ensure a high sample current, because finding the first electrons backscattered from the sample is expected to be much more difficult than in the straight-through mode normally used to tune the conventional EELS spectrometer. Because for most samples the intensity of the backscattered electrons entering the aperture of the analyser is far below the picoampere level, operation with a double-pass analyser is not realistic. Thus, for the present analyser, we adopted a single-pass CDA with a  $107.5^\circ$  deflection angle and a 1.5-fold magnified mean radius compared with that of the CDAs in the monochromator. The enlarged slit of the analyser increases the signal current by accepting a broadened electron beam due to aberrations without degrading the resolution of the analyser.

The geometrical design of the three-element acceleration lenses was determined by computer simulations of the electron trajectory using SIMION6 to minimize the image

of the exit slit of the monochromator at a sample position 240 mm away from the end of the acceleration lens system. The deceleration lenses have the same geometry and are placed symmetrically with respect to the centre axis of the octopole deflector. The axes of each lens are  $6^\circ$  away from the centre axis of the octopole and their crossing point is located at the sample position.

In order to have some additional adjusting parameters, we have included three small magnetic coils embedded in the entrance lens of the octopole deflector and in the acceleration and deceleration lenses. Although the effect on the beam focusing of these additional parameters is not so dramatic, these parameters work efficiently to trim the shape of the electron beam in some cases.

Because the trajectories of slow electrons are severely distorted by the inhomogeneous stray magnetic fields, care was taken to reduce the residual magnetic field in the spectrometer. The EELS part is doubly shielded by 'permalloy' tubes and each CDA is also covered by 'permalloy' housings. The octopole deflector is also shielded by a 'permalloy' tube. The residual magnetic field was measured to be  $<10$  mG in the EELS chamber and  $<70$  mG in the octopole deflector. Some elements of the acceleration and deceleration lenses are also made of 'permalloy' to shield the CDA parts from the magnetic field generated by small magnetic coils embedded in these lenses.

The main part of the EELS controller consisted of a combination of high-precision d.c. voltage generators and high-precision potentiometers. All the voltages are tuned and preadjusted with respect to the filament voltage and then all the electrode voltages are modified by the same value with respect to the sample potential to change the primary energy of the electron beam. Sample potential is set to the ground level. The electron energy loss spectra are taken by scanning the offset voltage of the analyser part with respect to the filament voltage via a programmable d.c. voltage generator (R6145: Advantest) controlled by a personal computer. The angular scanning is controlled by a 16-bit digital-to-analogue convertor mounted on a second personal computer. The electrons are counted by a standard pulse-counting system using a channel electron multiplier, a preamplifier and counters mounted on each personal computer. The energy-loss spectrum and the angular profile (LEED pattern) are thus recorded on the different personal computers independently. Radio frequency noise and a.c. components from the electronics are minimized by resistance-capacitance filters placed before the feedthroughs. The measured peak-to-peak noise levels of the electrode voltages supplied to the spectrometer were  $\sim 1$  mV.

Figure 2 shows the result of a LEED two-dimensional scan from the Si(111)- $7 \times 7$  surface. The sample was flashed at  $1230^\circ\text{C}$  for a few seconds in an ultrahigh vacuum ( $1 \times 10^{-10}$  Torr base pressure) for cleaning, and then annealed at  $800^\circ\text{C}$  for a few minutes to increase the long-range order of the surface atomic structure. The electrons were energy-filtered to 50 meV full width at half-maximum (FWHM). The primary energy of the electron beam was 50.3 eV, which was close to an out-of-phase (destructive) condition in LEED for the Si(111) neighbouring terraces. A sharp LEED pattern was obtained with a very high count rate of more than  $10^6$  cps at the (00) spot. Because the intensity is shown on a logarithmic scale and the scattering condition is nearly out of phase, a weak

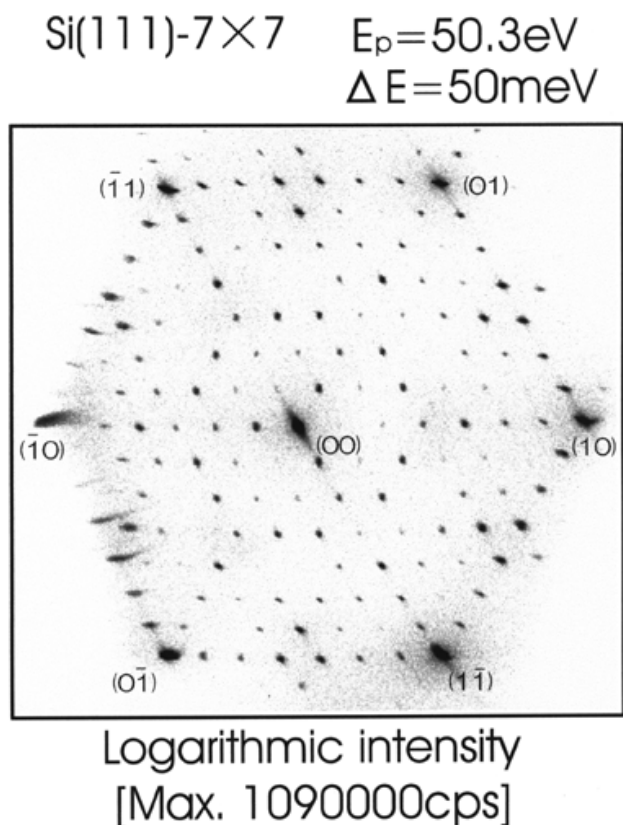
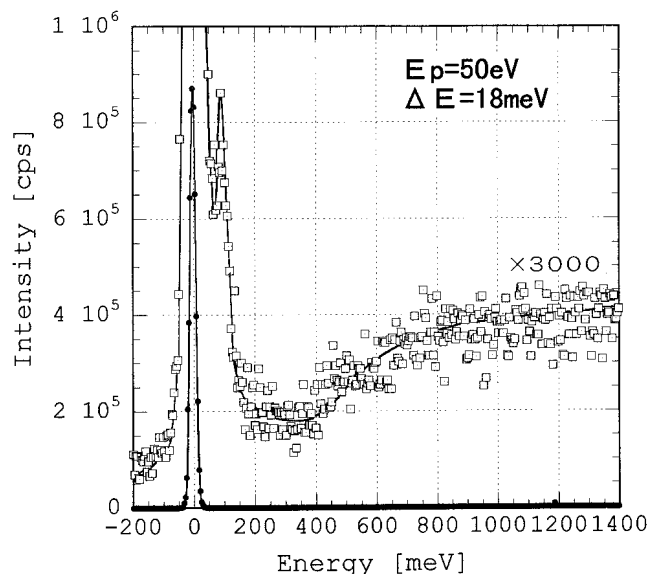


**Figure 2.** A two-dimensional LEED pattern of the Si(111)-7 × 7 surface taken at 50.3 eV primary energy and an energy filtering of 50 meV. Intensity is shown on a logarithmic scale. The (00) spot has a high intensity of  $1.09 \times 10^6$  cps.

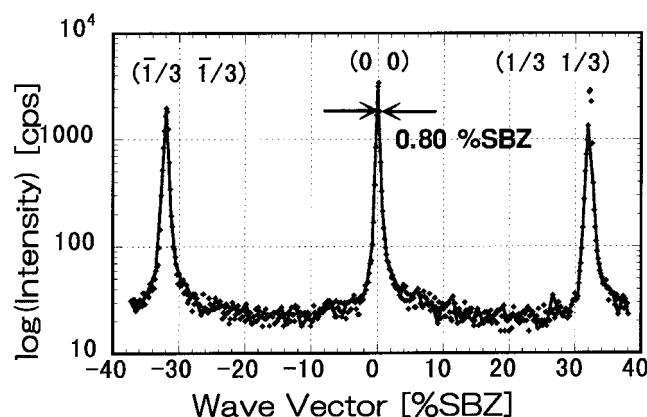
streaky feature in the (00) spot running from the (00) to the  $(\bar{1}1)$  direction is visible. This feature is assigned to sparsely distributed steps due to a slight ( $<0.3^\circ$ ) miscut angle of the wafer from the (111) direction. When we decrease the energy half-width of the electron beam, the intensity ratio of the background to the Bragg spots decreases, as well as the intensity of the Bragg spots themselves. This means a reduction in the background due to thermal diffuse scattering.

Figure 3 shows an electron energy-loss spectrum taken with the same surface at an (00) spot with 50 eV primary energy. The measured FWHM of the centre peak was 18 meV. Because the pass energy of the spectrometer was 1 eV, the theoretically expected energy resolution is 12 meV,<sup>19</sup> which is  $\sim 30\%$  smaller than the observed value. The larger energy half-width in this experiment will be attributed partly to scattering of low-frequency plasmons on Si(111), which is known to broaden the centre peak. The squares show the spectrum magnified by 3000 times. At  $\sim 90$  meV we can see a sharp feature attributed to a small amount of oxygen adsorbate due to residual oxygen or water dissociation. At higher loss energies of  $\sim 800$  meV the background gradually increases, which can be assigned to some interband transitions.

Figure 4 demonstrates the LEED one-dimensional scan taken with Si(111)- $\sqrt{3} \times \sqrt{3}$ -Ag along the (11) to the (00) direction at 55.0 eV primary energy. One fundamental and two super-reflection spots are seen. The FWHM of the (00) spot was 0.80% of the surface Brillouin zone. At a lower primary energy of 12.3 eV, as shown in Fig. 5,



**Figure 3.** Energy-loss spectrum at the (00) spot of the same Si(111)-7 × 7 surface as in Fig. 2, but after a 10 h lapse in an ultrahigh vacuum. Squares are magnified data points by 3000 times. The energy half-width at the centre peak is 18 meV (FWHM). A feature at  $\sim 90$  meV is attributed to adsorbed oxygen species originating from the residual gas.



**Figure 4.** An example of a one-dimensional LEED pattern taken at an electron primary energy of 55 eV. The surface is Si(111)- $\sqrt{3} \times \sqrt{3}$ -Ag.

the FWHM of the (00) spots narrows to 0.40% of the surface Brillouin zone ( $0.0065 \text{ \AA}^{-1}$ ). This is because the broadening of the (00) rod due to a mosaic structure becoming smaller at lower electron primary energies. The half-width of  $0.0065 \text{ \AA}^{-1}$  corresponds to a transfer width of  $960 \text{ \AA}$ , and the momentum resolution of the apparatus should be better than this value. The momentum resolution around  $1000 \text{ \AA}$  is comparable to that of the commercial SPA-LEED.

Other examples of two-dimensional LEED patterns taken at a primary energy of 132 eV are shown in Fig. 6. These data are taken in a single sequence of Ag depositions onto a vicinal Si(111) surface. The miscut angle is  $\sim 4^\circ$  toward the  $[1\bar{1}2]$  or the  $[\bar{1}12]$  from the (111) direction. After flashing the surface, a  $7 \times 7$  pattern was observed. Because the pattern is shown in a logarithmic intensity scale, which displays more clearly the weak features due to surface morphology, sharp streaks running in the direction of the miscut angle are seen at the position

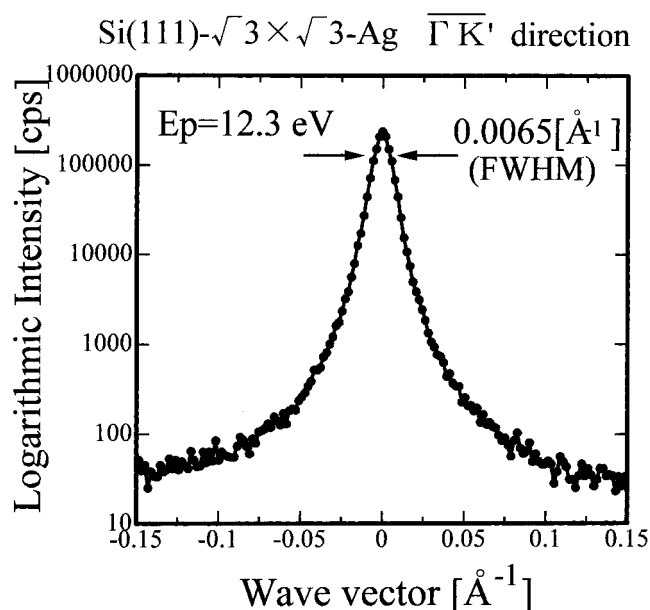


**Figure 5.** One-dimensional LEED pattern around a (00) spot taken from the same surface as in Fig. 4. Scanning direction is (00)–(11). Primary energy is 12.3 eV. The momentum resolution is  $0.0065 \text{ \AA}^{-1}$ , which corresponds to a transfer width of  $960 \text{ \AA}$ .

of Bragg spots. This feature corresponds to a narrow width ( $\sim 40 \text{ \AA}$ ) of the (111) terraces with  $7 \times 7$  reconstruction on them. After depositing a submonolayer of Ag and annealing at  $\sim 580^\circ\text{C}$ , the surface shows a  $\sqrt{3} \times \sqrt{3}$ -Ag pattern with some associated streaks. After further Ag deposition, the streaks almost disappear and only a sharper  $\sqrt{3} \times \sqrt{3}$ -Ag pattern is observed. The width of the elongated features decreases as the Ag coverage increases

(not shown here), which is indicative of an increase in the terrace width, or the appearance of bunched steps.

## SUMMARY

We have constructed a new version of an ELS-LEED that is a combination of an Ibach-type double-pass monochromator and a octopole electrostatic deflection unit. In preliminary tests using an Si(111)- $7 \times 7$  surface, the spectrometer showed a high signal intensity of  $\sim 10^6$  cps with a moderate energy resolution better than 20 meV. A high momentum resolution of  $0.0065 \text{ \AA}^{-1}$ , which corresponds to a transfer width of  $\sim 1000 \text{ \AA}$ , was achieved. With a proper sample and operating at a lower pass energy of the spectrometer, the apparatus is expected to show better energy resolution. Some plasmon dispersion measurements utilizing the high momentum resolution of this new version of ELS-LEED are now in progress (details available from the author upon request).

## Acknowledgements

T. N. is deeply indebted to Professors M. Henzler and C. Oshima for valuable discussions and their continuous encouragement in the present study. He is also grateful to B. Gottschlich (Omicron Vakuumphysik GmbH), T. Hildebrandt, H. Frischat and F.-J. Meyer zu Heringdorf for technical discussions. This work has been supported in part by Grants-in-Aid from the Ministry of Education, Science, Culture, and Sports of Japan, especially through the Grants-in-Aid for Creative Basic Scientific Research (No. 08NP1201) conducted by Professor K. Yagi of the Tokyo Institute of Technology. T. N. is also supported by the Nippon Sheet Glass Foundation for Materials Science and Engineering.

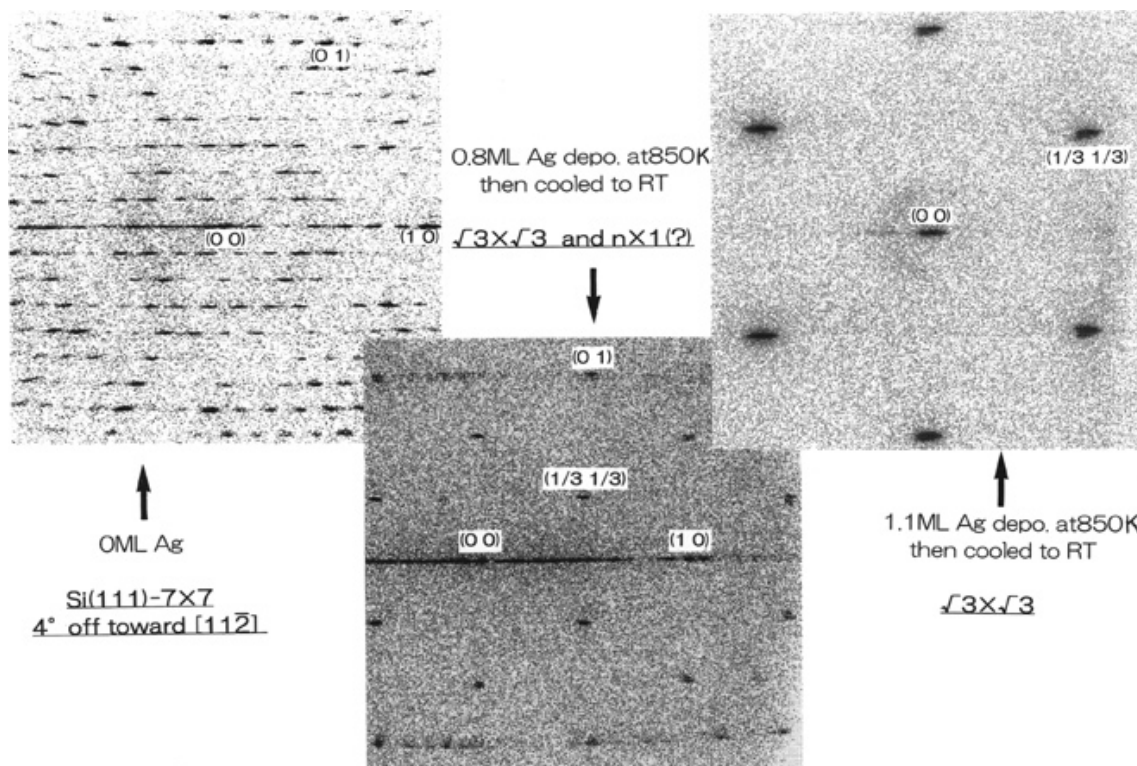


**Figure 6.** Evolution of the diffraction pattern with Ag deposition accompanied by subsequent annealing. The miscut angle of the Si(111) sample is  $\sim 4^\circ$ . The elongated diffuse feature of the spots is due to the narrow terrace width.

## REFERENCES

1. Henzler M. In *Electron Spectroscopy for Surface Analysis*, Ibach H (ed.). Springer-Verlag: Berlin, 1977; 117–149.
2. Van Hove MA, Tong SY. *Surface Crystallography by LEED: Theory, Computation, and Structural Results*. Springer-Verlag: Berlin, 1979.
3. Pendry JB. *Low Energy Electron Diffraction: the Theory and its Application to Determination of Surface Structure*. Academic Press: New York, 1974.
4. Henzler M. In *Dynamic Phenomena at Surfaces, Interfaces and Superlattices*, Nizzoli F, Rieder K-H, Willis RF (eds). Springer-Verlag: Berlin, 1985; 14.
5. Ibach H, Mills DL. *Electron Energy Loss Spectroscopy and Surface Vibration*. Academic Press: New York, 1982.
6. Palmer RE, Rous PJ, Wilkes JL, Willis RF. *Phys. Rev. Lett.* 1988; **60**: 329.
7. Tsuei K-D, Plummer EW, Liebsch A, Kempa K, Bakshi P. *Phys. Rev. Lett.* 1990; **64**: 44.
8. Rocca M, Valbusa U. *Phys. Rev. Lett.* 1990; **64**: 2398.
9. Nagao T, Kitamura K, Iizuka Y, Oshima C. *Surf. Sci.* 1993; **290**: 436.
10. Nagao T, Iizuka Y, Shimazaki T, Oshima C. *Phys. Rev. B* 1997; **55**: 10064.
11. Thiry PA, Liehr M, Pireaux JJ, Caudano R. *Surf. Sci.* 1987; **189/190**: 373.
12. Noguchi M, Hirakawa K, Ikoma T. *Phys. Rev. Lett.* 1991; **66**: 2243.
13. Tsuruoka T, Sekoguchi M, Uehara Y, Ushioda S, Kojima T, Ohta K. *Phys. Rev. B* 1994; **50**: 2346.
14. Nagao T, Voges C, Tsuchie K, Klos G, Pfner H, Henzler M, Ino S, Hasegawa S. *Phys. Rev. B* 1998; **57**: 10100.
15. Nakajima Y, Voges C, Nagao T, Hasegawa S, Klos G, Pfner H. *Phys. Rev. B* 1997; **55**: 8129.
16. Claus H, Buessenschuett A, Henzler M. *Rev. Sci. Instrum.* 1992; **63**: 2195.
17. Moresco F, Rocca M, Zielasek V, Hildebrandt T, Henzler M. *Phys. Rev. B* 1996; **54**: R14333.
18. Hildebrandt T. *Dissertation*, Hannover, Germany, 1999.
19. Ibach H. *Electron Energy Loss Spectrometers*. Springer-Verlag: Berlin, 1991; 41.
20. Nagao T, Iizuka Y, Umeuchi M, Shimazaki T, Nakajima M, Oshima C. *Rev. Sci. Instrum.* 1993; **65**: 515.